

# Comparison of neutralino and sneutrino dark matter in a model with spontaneous CP violation

---

Katri Huitu,<sup>a</sup> Jari Laamanen,<sup>b</sup> Lasse Leinonen,<sup>a</sup> Santosh Kumar Rai,<sup>c</sup> Timo R uppell<sup>a</sup>

<sup>a</sup>*Department of Physics, and Helsinki Institute of Physics, FIN-00014 University of Helsinki, Finland*

<sup>b</sup>*Theoretical High Energy Physics, IMAPP, Faculty of Science, Radboud University Nijmegen, Mailbox 79, P.O. Box 9010, NL-6500 GL Nijmegen, The Netherlands*

<sup>c</sup>*Department of Physics and Oklahoma Center for High Energy Physics, Oklahoma State University, Stillwater, OK 74078, USA*

*E-mail:* [katri.huitu@helsinki.fi](mailto:katri.huitu@helsinki.fi), [j.laamanen@science.ru.nl](mailto:j.laamanen@science.ru.nl),  
[lasse.leinonen@helsinki.fi](mailto:lasse.leinonen@helsinki.fi), [santosh.raiookstate.edu](mailto:santosh.raiookstate.edu),  
[timo.ruppell@helsinki.fi](mailto:timo.ruppell@helsinki.fi)

**ABSTRACT:** Supersymmetric extensions to the standard model provide viable dark matter candidates and can introduce additional charge-parity (CP) violation needed for obtaining the observed baryon asymmetry of the universe. We study the possibilities of scalar and neutralino dark matter with spontaneous CP violation in the next-to-minimal supersymmetric standard model with a right-handed neutrino. The observed relic density can be produced both by a neutralino or a right-handed sneutrino as the lightest supersymmetric particle but when CP is violated new annihilation channels become available and in general lower the relic density. We consider collider phenomenology for a number of benchmark points which all satisfy experimental constraints and have either the neutralino or the right-handed sneutrino contribute to the dark matter abundance.

**KEYWORDS:** CP violation, Dark Matter

ARXIV EPRINT: [1209.6302](https://arxiv.org/abs/1209.6302)

---

## Contents

<b>1</b>	<b>Introduction</b>	<b>1</b>
<b>2</b>	<b>NMSSM with a singlet neutrino superfield</b>	<b>3</b>
<b>3</b>	<b>Constraints and the parameter space</b>	<b>5</b>
3.1	Parameters	5
3.2	Tools	5
3.3	Constraints	6
<b>4</b>	<b>The effects of SCPV on the relic density and other constraints</b>	<b>8</b>
<b>5</b>	<b>Direct dark matter searches</b>	<b>12</b>
<b>6</b>	<b>Signatures at the colliders</b>	<b>13</b>
<b>7</b>	<b>Summary and discussion</b>	<b>17</b>
<b>8</b>	<b>Acknowledgments</b>	<b>18</b>

---

## 1 Introduction

One of the most compelling hints of physics beyond the standard model is the cosmological observation that more than 80 % of the mass of the universe is composed of dark matter (DM) [1]. This evidence comes both from the astronomical observations of gravitational effects at various scales and the cosmic microwave background measurements which are consistent with such a large amount of dark matter.

Supersymmetry (SUSY) is one of the prime candidates of new physics and may provide an appropriate dark matter particle. Supersymmetric models generally contain terms, which violate baryon and lepton number conservation, and potentially lead to fast proton decay. The presence of such terms can be prevented by conservation of  $R$ -parity [2–6]. The remarkable consequence of  $R$ -parity conservation is that the lightest supersymmetric particle (LSP) will be absolutely stable. The LSPs left over after the Big Bang could then explain the observed dark matter relic density (RD). The LSP is thought to be uncharged (in both electric and color charges) so it interacts only weakly or through gravitational interactions.

The candidates for the lightest supersymmetric particle in the minimal supersymmetric extension of the standard model (MSSM) spectrum are the lightest neutralino, gravitino, and sneutrino. The LEP-collider searches exclude a light left-handed sneutrinos as the LSP, and masses beyond LEP’s reach are ruled out by direct detection searches [7–10]. However,

the superpartner of the right-handed neutrino is a viable dark matter candidate [11, 12]. A pure right-handed (RH) sneutrino has a very reduced coupling to ordinary matter due to the smallness of the neutrino Yukawa coupling and is therefore not produced thermally in the early universe. If, however, the right-handed sneutrino is by other means coupled to the rest of the observable sector it may be a thermal relic and provide for an appropriate dark matter relic density.

Supersymmetry must be a broken symmetry at low energies. The explicit SUSY breaking is introduced softly so that no quadratic divergences appear. This requires inclusion of all the possible gauge invariant breaking terms in the Lagrangian. The large number of breaking parameters parametrize the supersymmetry breaking, which is expected to be spontaneous in a more complete theory. Soft SUSY breaking introduces a large number of complex phases, which can lead to large CP violation effects [13]. While cosmological observations of the baryon asymmetry of the universe suggest that additional CP violation beyond what the Standard Model (SM) offers is necessary [14], SUSY phases typically produce excessively large electric dipole moments (EDMs) [15, 16]. One way to manage this problem is to impose CP conservation on the Lagrangian and introduce spontaneous CP violation (SCPV) [17]. SCPV is an attractive solution since it radically decreases the number of free CP-violating parameters, in addition to allowing study of the interplay between different CP observables [18]. It is well known that SCPV is not possible in the MSSM and requires at least one and preferably two additional singlet fields [19, 20]. Therefore, we are led to consider SCPV in the next-to-minimal standard model (NMSSM).

The NMSSM [21–23] provides also a solution to the so-called  $\mu$  problem [24] by introducing an extra singlet scalar superfield  $\hat{S}$  (lepton number  $L = 0$ ), whose vacuum expectation value (vev) will generate an effective  $\mu$  term. This naturally leads to  $\mu$  to be of the order of the electroweak (EW) scale. The singlet also contributes to the Higgs masses already at the tree-level, which may lead to heavier Higgses than in the MSSM. Adding yet another singlet superfield  $\hat{N}$  ( $L = 1$ ) to the NMSSM provides for right-handed neutrino and sneutrino states. Since both  $\hat{S}$  and  $\hat{N}$  are gauge singlets it is tempting to have one field to do the job of both. This, however, leads to fine tuning problems as well as either explicit  $R$ -parity violation or spontaneous lepton number violation with a superfluous Goldstone boson in the spectrum [25]. Therefore, both singlets are assumed to be included in the model. Interestingly, a non-vanishing vev of the superfield  $\hat{S}$  enables an effective Majorana mass term for the right-handed neutrino similar to the effective  $\mu$  term. Moreover, the presence of the singlet  $\hat{S}$  also leads to the electroweak scale interactions of the right-handed sneutrino with other MSSM fields.

In this work we study neutralino and right-handed sneutrino dark matter in the framework of an extended NMSSM when CP is spontaneously violated. For the case of no CP violation, the possible right-handed sneutrino dark matter in the NMSSM has been earlier investigated in [26, 27] and neutralino dark matter in [28, 29]. Here we first introduce the changes in the model due to the spontaneous CP violation. We scan over interesting ranges for a number of parameters. After taking into account all relevant experimental constraints it is seen that CP violation decreases the dark matter relic density because of new available decay channels. The possible collider signals are considered for several benchmark points,

two of which have a sneutrino as an LSP and five of which have a neutralino LSP.

## 2 NMSSM with a singlet neutrino superfield

We start by introducing the important properties of the model. The superpotential for the NMSSM with singlet superfields  $\hat{S}$  (L=0) and  $\hat{N}$  (L=1) is given by

$$W = \epsilon_{\alpha\beta} \left( Y_E^{ij} \hat{H}_1^\alpha \hat{L}_i^\beta \hat{E}_j + Y_D^{ij} \hat{H}_1^\alpha \hat{Q}_i^\beta \hat{D}_j + Y_U^{ij} \hat{Q}_i^\alpha \hat{H}_2^\beta \hat{U}_j + Y_N^i \hat{L}_i^\alpha \hat{H}_2^\beta \hat{N} + \lambda \hat{S} \hat{H}_2^\alpha \hat{H}_1^\beta \right) + \lambda_N \hat{N} \hat{N} \hat{S} + \frac{\kappa}{3} \hat{S} \hat{S} \hat{S}, \quad (2.1)$$

where  $\epsilon_{\alpha\beta}$  ( $\alpha, \beta = 1, 2$ ) is a totally antisymmetric tensor with  $\epsilon_{12} = 1$ ,  $\hat{X}$  denotes a superfield and the rest are dimensionless couplings. The soft SUSY breaking terms are

$$V_{\text{soft}} = \left\{ \epsilon_{\alpha\beta} \left( A_E^{ij} Y_E^{ij} H_1^\alpha \tilde{L}_i^\beta \tilde{E}_j + A_D^{ij} Y_D^{ij} H_1^\alpha \tilde{Q}_i^\beta \tilde{D}_j + A_U^{ij} Y_U^{ij} \tilde{Q}_i^\alpha H_2^\beta \tilde{U}_j + A_N^i Y_N^i \tilde{L}_i^\alpha H_2^\beta \tilde{N} + A_\lambda \lambda S H_2^\alpha H_1^\beta \right) + A_{\lambda_N} \lambda_N \tilde{N} \tilde{N} S + \frac{A_\kappa \kappa}{3} S S S + \xi^3 S \right\} + \text{h.c.} \\ + M_{\Phi,ij}^2 \Phi_i^\dagger \Phi_j + M_{\Theta,ij}^2 \Theta_i \Theta_j^* + m_{H_1}^2 H_1^\dagger H_1 + m_{H_2}^2 H_2^\dagger H_2 + m_S^2 S S^*, \quad (2.2)$$

where  $\Phi = \{\tilde{L}, \tilde{Q}\}$ ,  $\Theta = \{\tilde{E}, \tilde{N}, \tilde{U}, \tilde{D}\}$  are the scalar components of the corresponding superfields. A discussion on the theoretical merits of this and similar models (specifically the soft  $S$  tadpole) can be found in [23, 30, 31]. For phenomenological merits of this and similar models (NMSSM + right-handed neutrino) see [32–34].

In this work we take only the third generation Yukawa couplings to be non-zero for  $Y_{U/D/E}$  and impose at the electroweak scale  $Y_N^i = Y_N$  and  $A_N^i = A_N$  for all three generations. We also take all soft scalar masses diagonal,  $M_{ij}^2 = M^2 \delta_{ij}$ , and take  $M_U = M_D = M_Q$ , as well as  $M_E = M_L$ . It is worth pointing out a tension in choosing natural sizes for some of these parameters. If we want the  $\mu$  problem solved then  $\langle S \rangle \sim \text{EW scale}$  and it follows that  $M_N \sim \langle S \rangle \sim \text{EW scale}$ , assuming that  $\lambda$  and  $\lambda_N$  are  $\mathcal{O}(1)$ . Now the left-handed neutrino masses are generated by the conventional seesaw mechanism:

$$M_\nu = \begin{pmatrix} 0 & m_D \\ m_D^T & M_N \end{pmatrix} \rightarrow m_{\nu_L} \simeq -m_D M_N^{-1} m_D^T, \quad (2.3)$$

where  $m_D \sim Y_N \times \text{EW scale}$  and thus  $m_{\nu_L} \sim Y_N^2 \times \text{EW scale}$ , meaning we need to choose  $Y_N \sim 10^{-6}$ . Otherwise, even for  $\langle S \rangle \sim M_N \sim M_{\text{Planck}}$  we would have  $Y_N \sim 10^{-2}$  on top of which we would have to choose  $\lambda \sim 10^{-17}$ .

Spontaneous CP violation is introduced by complex vacuum expectation values of the  $S$  and  $H_2^0$  fields,

$$\langle H_2 \rangle = \begin{pmatrix} 0 \\ v_2 e^{i\delta_2} \end{pmatrix}, \quad \langle S \rangle = v_S e^{i\delta_S}. \quad (2.4)$$

A complex phase of the vev of  $H_1^0$  can be absorbed by field redefinitions ( $\langle H_1^0 \rangle = v_1$ ). Non-zero vevs for left- or right-handed sneutrinos would introduce spontaneous R-parity breaking. Since we are interested in viable dark matter candidates we consider only R-parity conserving models. Thus there are only two complex phases  $\delta_S$  and  $\delta_2$  which enter

couplings and mass matrices wherever the vevs of  $S$  and  $H_2^0$  appear. In particular the mass matrices of neutral scalars are no longer block diagonal with respect to the division of CP even and CP odd gauge eigenstates. The sneutrinos form an  $8 \times 8$  mass matrix divided into  $4 \times 4$  submatrices

$$M_{\tilde{\nu}}^2 = \begin{pmatrix} m_{ee}^2 & m_{eo}^2 \\ m_{oe}^2 & m_{oo}^2 \end{pmatrix} \quad (2.5)$$

where the subscript denotes CP-even/odd states. We introduce the following notation

$$A_i^{\pm\pm} = Y_N^i (A_N^i v_2 \cos \delta_2 \pm 2\lambda_N v_2 v_S \cos(\delta_2 - \delta_S) \pm \lambda v_1 v_2 \cos \delta_S), \quad (2.6)$$

$$B_i^{\pm\pm} = A_i^{\pm\pm} (\cos \rightarrow \sin), \quad (2.7)$$

$$C^{\pm\pm} = 2\lambda_N A_{\lambda_N} v_S \cos \delta_S \pm 2\kappa \lambda_N v_S^2 \cos 2\delta_S \pm 2\lambda \lambda_N v_1 v_2 \cos \delta_2, \quad (2.8)$$

$$D^{\pm\pm} = C^{\pm\pm} (\cos \rightarrow \sin), \quad (2.9)$$

$$m_{L,ij}^2 = M_{L,ij}^2 + Y_N^i Y_N^j (v_1^2 + v_2^2) + \frac{1}{2} m_Z^2 \cos 2\beta \delta_{ij}, \quad (2.10)$$

$$m_R^2 = M_N^2 + \sum_i Y_N^{i2} (v_1^2 + v_2^2) + 4\lambda_N^2 v_S^2. \quad (2.11)$$

The  $4 \times 4$  submatrices are then

$$m_{ee}^2 = \begin{pmatrix} m_{L,ij}^2 & A_i^{+-} \\ A_j^{+-} & m_R^2 + C^{+-} \end{pmatrix}, \quad m_{oo}^2 = \begin{pmatrix} m_{L,ij}^2 & A_i^{--} \\ A_j^{--} & m_R^2 - C^{+-} \end{pmatrix}, \quad (2.12)$$

$$m_{oe}^2 = \begin{pmatrix} 0_{3 \times 3} & -B_i^{++} \\ B_j^{-+} & D^{-+} \end{pmatrix}, \quad m_{eo}^2 = (m_{oe}^2)^T. \quad (2.13)$$

where  $i, j$  are the family indices of the left-handed sneutrinos. The mixing between left- and right-handed sneutrino states is suppressed by the smallness of neutrino Yukawa  $Y_N$  in  $A^{\pm\pm}$  and  $B^{\pm\pm}$ . The CP-violating mixing between even and odd states by  $B^{\pm\pm}$  can be further suppressed if the CP-violating phases are small. There is no mixing between even and odd left-handed states and the mass splitting for left-handed states is proportional to  $Y_N^2$ . Consequently our model has almost purely left-handed mass degenerate sneutrinos which are CP eigenstates to a high degree of accuracy.

The dominantly right-handed sneutrinos are split by  $C^{+-}$  and  $D^{-+}$  into

$$m_{\tilde{\nu}_{1,2}}^2 \simeq m_R^2 \mp \sqrt{C^{+-2} + D^{-+2}}. \quad (2.14)$$

From Eqs. (2.8) and (2.9) we see that the mass splitting is proportional to  $\lambda_N$  but unsuppressed by possibly small CP phases due to the complimentary nature of  $C^{+-}$  and  $D^{-+}$  with respect to the CP-violating phases. The mixing between even and odd states is done by  $D^{-+}$  which may be suppressed by small CP violating phases.

The Higgs mass matrix is also no longer block diagonal but becomes a  $6 \times 6$  matrix where the CP-even and CP-odd states mix. The usual vacuum stability conditions are solved for the EW scale mass parameters  $m_{H_1}$ ,  $m_{H_2}$ , and  $m_S$ . The addition of CP phases introduces new vacuum stability conditions which we solve by fixing the soft trilinear terms

$A_\lambda$  and  $A_\kappa$ . At tree level

$$\frac{\partial V}{\partial \delta_2} = 0 \rightarrow A_\lambda = -\kappa v_S \frac{\sin(\delta_2 - 2\delta_S)}{\sin(\delta_2 + \delta_S)}, \quad (2.15)$$

$$\frac{\partial V}{\partial \delta_S} = 0 \rightarrow A_\kappa = -\frac{3\kappa\lambda v_1 v_2 v_S \sin(\delta_2 - 2\delta_S) + \xi^3 \sin \delta_S}{\kappa v_S^2 \sin 3\delta_S}. \quad (2.16)$$

In our numerical calculations we use the 1-loop effective scalar potential including the corrections from the third generation (s)quarks to derive both the mass matrices and the vacuum stability conditions.

The neutralino mass matrix is of the conventional NMSSM form with the addition of complex phases

$$M_{\chi^0} = \begin{pmatrix} M_1 & 0 & -\frac{g_1 v_1}{\sqrt{2}} & \frac{g_1 v_2}{\sqrt{2}} e^{-i\delta_2} & 0 \\ 0 & M_2 & \frac{g_2 v_1}{\sqrt{2}} & -\frac{g_2 v_2}{\sqrt{2}} e^{-i\delta_2} & 0 \\ -\frac{g_1 v_1}{\sqrt{2}} & \frac{g_2 v_1}{\sqrt{2}} & 0 & -\lambda v_S e^{i\delta_S} & -\lambda v_2 e^{i\delta_2} \\ \frac{g_1 v_2}{\sqrt{2}} e^{-i\delta_2} & -\frac{g_2 v_2}{\sqrt{2}} e^{-i\delta_2} & -\lambda v_S e^{i\delta_S} & 0 & -\lambda v_1 \\ 0 & 0 & -\lambda v_2 e^{i\delta_2} & -\lambda v_1 & 2\kappa v_S e^{i\delta_S} \end{pmatrix}. \quad (2.17)$$

### 3 Constraints and the parameter space

#### 3.1 Parameters

We carry out our numerical analysis of the effect of the CP-violating phases by randomly sampling the parameters that affect the Higgs and sneutrino spectra as well as the interactions of the dark matter candidate. The gaugino masses were left fixed to better illustrate the effect of bino dominance in the neutralino LSP. The parameters affecting squark masses were chosen such that we avoid the current experimental limits completely. We have generated two data sets, one CP-conserving ( $\delta_2 = \delta_S = 0$ ) and one where we vary the CP phases along with the other sampled parameters. Table 1 gives the values for the fixed parameters and the ranges for the sampled parameters.

#### 3.2 Tools

The computational tools we use are LanHEP [35] for model file creation and micrOmegas (v.2.4.1) for the main numerical analysis [36]. Calculating the spectrum and diagonalizations are performed using the EISPACK [37] routines and calculation of electric dipole moments and rare decay branching ratios is performed by a dedicated Mathematica code. B-physics constraints are calculated by NMSSMtools [38, 39] using the supplied NMSSM model.

There are two caveats to the use of NMSSMtools which we will briefly address here. One is that the NMSSM model does not include a right-handed neutrino. However, loop contributions to the calculation of  $\text{BR}(B \rightarrow X_s \gamma)$  and  $\text{BR}(B_s \rightarrow \mu^+ \mu^-)$  that involve a right-handed sneutrino will be suppressed by  $Y_N^2/Y_{\tau/\mu}^2$  compared to the corresponding left-handed contributions and are thus negligible in our model. The other caveat to using NMSSMtools is that CP violation is not implemented in the supplied NMSSM model. Two

$M_1$	300 GeV
$M_2$	600 GeV
$M_3$	1800 GeV
$M_Q$	1000 GeV
$A_t$	1500 GeV
$A_b$	1500 GeV
$A_\tau$	-2500 GeV
$Y_{N_i}$	$10^{-6}$
$A_{N_i}$	0 GeV

$\tan \beta$	2 – 50
$\mu$	0 – 500 GeV
$\lambda$	0 – 0.8
$\kappa$	0 – 0.8
$A_\lambda$	-1000 GeV – 1000 GeV
$A_\kappa$	-1000 GeV – 1000 GeV
$v_S$	$\mu/\lambda$
$\lambda_N$	0 – 0.8
$A_{\lambda_N}$	-1000 GeV – 1000 GeV
$M_N$	0 – 500 GeV
$M_{L,E}$	0 – 500 GeV
$\delta_S$	0 – $2\pi^*$
$\delta_2$	0 – $2\pi^*$
$\xi$	-1000 GeV – 1000 GeV

**Table 1.** The parameters and sampling ranges used in our two data sets. \*EDM considerations limit the range of the phases considerably and we use the ranges  $[0, 0.3]$ ,  $[\pi - 0.3, \pi + 0.1]$ , and  $[2\pi - 0.1, 2\pi]$  for generating points that are subject to all of the experimental constraints.

factors can affect the calculation: changes in the model’s spectrum due to non-zero CP phases, and changes in the couplings of the fields. For the particles appearing in the tree level and 1-loop contributions to  $\text{BR}(B \rightarrow X_s \gamma)$ ,  $\text{BR}(B^+ \rightarrow \tau^+ \nu_\tau)$ , and  $\text{BR}(B_s \rightarrow \mu^+ \mu^-)$ , the spectrum changes continuously from  $\delta_2, \delta_S = 0 \rightarrow \delta_2, \delta_S \neq 0$ . To judge the impact of CP phases on the calculations we did a comparative analysis using the MSSM for which both CP-conserving and CP-violating code bases exist in NMSSMtools. In the limit of small CP phases we find that the difference in the results for  $\text{BR}(B \rightarrow X_s \gamma)$ ,  $\text{BR}(B^+ \rightarrow \tau^+ \nu_\tau)$ , and  $\text{BR}(B_s \rightarrow \mu^+ \mu^-)$  is at the 5% level for phases as large as  $\pi/10$  and more generally at the level of 1% for phases  $< 0.1$ .

This gives us confidence that the CP-conserving NMSSM model can be used to calculate  $B$ -physics constraints in the regime of small CP-violating phases ( $\delta_2, \delta_S < 0.1$ ). Satisfying the EDM constraints restricts us naturally to this regime. We find that in our CP-violating data set most points that satisfy EDM constraints have  $|\delta_2| < 0.05$  (modulo  $\pi$ ). The phase  $\delta_S$  is not as constrained and in general the phases  $\delta_2$  and  $\delta_S$  can both have large values such that the physical phases entering EDM calculations are fine tuned to be small. However, to simplify calculations and to be able to use the NMSSMtools package mentioned above we restrict both phases to the ranges  $[0, 0.3]$ ,  $[\pi - 0.3, \pi + 0.1]$ , and  $[2\pi - 0.1, 2\pi]$  when generating points that are subjected to all the experimental constraints we impose.

### 3.3 Constraints

In order to examine only physically relevant parameter regions, a number of constraints are taken into account during our computations. We check the scalar sector for vacuum stability and the sparticle spectrum against the most recent PDG limits [40].

The LEP experiment places the lower limit on the standard model Higgs boson mass at 114 GeV. As the Higgs boson can only be detected by its decay products, not directly, a model independent way to use the experimental results is to investigate the bounds on Higgs boson couplings to  $ZZ$  and  $hZ$ . In the NMSSM the couplings  $hZZ$  and  $hhZ$  may differ from the standard model and consequently the mass of the Higgs boson can be below 114 GeV, provided that the couplings are sufficiently small. The reduced  $Z$  couplings are

$$g_{h_i ZZ} = \cos \beta \mathcal{O}_{1i} + \sin \beta \mathcal{O}_{2i} \quad (3.1)$$

$$g_{h_i h_j Z} = (\sin \beta \mathcal{O}_{4i} + \cos \beta \mathcal{O}_{5i})(\cos \beta \mathcal{O}_{2j} - \sin \beta \mathcal{O}_{1j}) - (i \rightarrow j) \quad (3.2)$$

with  $\mathcal{O}_{ij}$  the  $6 \times 6$  neutral Higgs mixing matrix. We use the most recent limits these couplings impose on the Higgs mass, which are presented in [41]. The recent results from the LHC and Tevatron experiments imply that the SM-like Higgs boson mass should be around  $m_H \sim 125$  GeV [42, 43]. In our analysis we thus also require one of the Higgs states to have a mass between 123 – 128 GeV. The 125 GeV Higgs signal in the NMSSM has recently been studied in Refs. [44–47].

The phases  $\delta_2$  and  $\delta_5$  that introduce CP violation in our model are flavor diagonal and thus are expected to be highly constrained from, e.g, the electron electric dipole moment measurements. Current limits [48] constrain the electron EDM to be below

$$d_e < 1.05 \cdot 10^{-27} \text{ ecm}. \quad (3.3)$$

The NMSSM specific contributions to  $\text{BR}(B \rightarrow X_s \gamma)$  from the extended Higgs and neutralino sectors arise only at two-loop level [23] and, in general, are considered to be small [49, 50]. In our calculations, the theoretical uncertainties [51, 52] are combined with the present experimental value [53], which leads to [54]

$$\text{BR}(B \rightarrow X_s \gamma) = (355 \pm 142) \times 10^{-6}. \quad (3.4)$$

The impact of the NMSSM on the branching ratio  $\text{BR}(B^+ \rightarrow \tau^+ \nu_\tau)$  is only indirect, and the extra singlet contributions are suppressed by the small neutrino Yukawas as mentioned earlier. The new physics contribution to the branching ratio can be quantified by defining a ratio [55, 56]

$$0.99 < \frac{\text{BR}(B^+ \rightarrow \tau^+ \nu_\tau)_{\text{SM+SUSY}}}{\text{BR}(B^+ \rightarrow \tau^+ \nu_\tau)_{\text{SM}}} < 3.19, \quad (3.5)$$

where the numerator denotes the branching ratio in the SUSY scenario. The constraint (3.5) tends to prefer small values of  $\tan \beta$  in order not to decrease the ratio too much below the lower limit. A large charged Higgs mass decreases the new physics contributions in general.

The effect of our model on  $\text{BR}(B_s \rightarrow \mu^+ \mu^-)$  at one loop comes from right-handed (s)neutrinos and is thus suppressed by the smallness of the neutrino Yukawa coupling. We apply the limit from [57]

$$\text{BR}(B_s \rightarrow \mu^+ \mu^-) < 4.5 \cdot 10^{-9} \quad (3.6)$$



The anomalous magnetic moment of the muon has been measured quite precisely. However, there is uncertainty in the reliability of the theoretical prediction due to hadronic and non-perturbative effects. Therefore, we do not use the magnetic moment as a constraint.

The relic density of cold dark matter in the universe is determined by the Wilkinson Microwave Anisotropy Probe (WMAP) [1] to be  $\Omega_c h^2 = 0.1126 \pm 0.0036$ . If 10 % theoretical uncertainty is added [58] we find the preferred WMAP range

$$0.0941 < \Omega_c h^2 < 0.1311 \quad (3.7)$$

at  $2\sigma$  level. As the dark matter may also contain a component of a non-supersymmetric origin, we have used only the upper bound as a constraint.

#### 4 The effects of SCPV on the relic density and other constraints

In this section we show the effects of CP violation on the relic density of the LSP. All plots contain points from the CP-violating data set unless otherwise specified. All points also satisfy PDG constraints on the mass spectrum and vacuum stability.

Spontaneous CP violation is known to change the spectrum of the scalar sector in a discontinuous manner. For small values of the phases there appears a light state,  $h_S$ , in the spectrum [59]. Experimental constraints on the Higgs boson mass force this light state to be singlet dominated [41]. We define the doublet content of  $h_S$  as

$$\epsilon_{sd} = \sum_{i=1,2,4,5} \mathcal{O}_{i2}^2 \quad (4.1)$$

with  $\mathcal{O}$  the neutral Higgs mixing matrix and the free index  $i$  runs over the elements corresponding to the lightest Higgs' gauge eigenstates separated into CP-even and CP-odd parts, i.e.  $\{\text{Re}H_1^0, \text{Re}H_2^0, \text{Re}S, \text{Im}H_1^0, \text{Im}H_2^0, \text{Im}S\}$ . We find that for our data points the value of  $\epsilon_{sd}$  is between  $0.1 - 10^{-5}$ . The presence of this light singlet state has different effects depending on what kind of LSP we have.

The addition of the singlet to the model also opens up the possibility for the neutralino LSP to have a significant singlino admixture and thus behave differently from its usual MSSM counterpart. We denote the singlino component of the neutralino LSP as

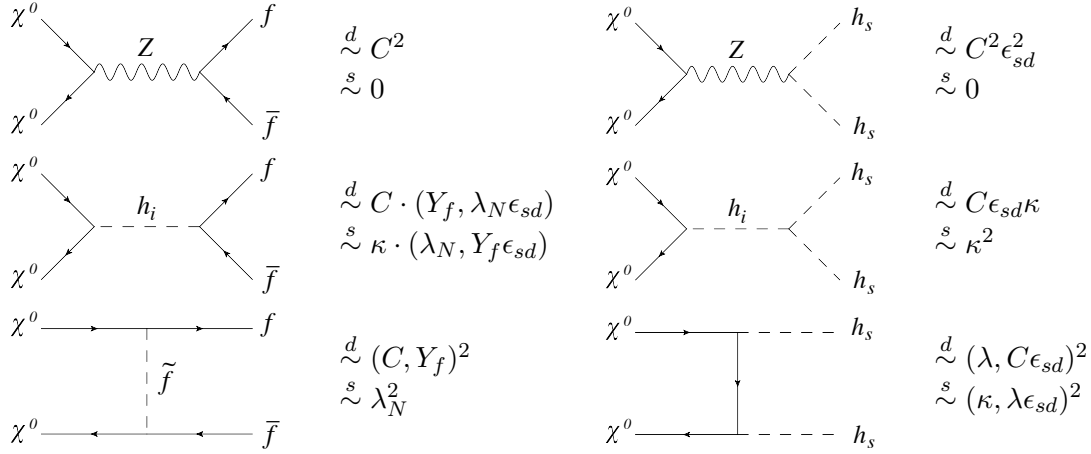
$$\epsilon_{\chi s} = |N_{51}|^2, \quad (4.2)$$

where  $N$  is the neutralino mixing matrix. We find that already at values of 0.1 the behavior of, e.g., the relic density of the neutralino depends significantly on the Lagrangian parameters associated with the singlino.

The other masses in the spectrum are also affected by the CP phases, but in a continuous way, meaning that for small values of the phases the spectrum is very close to the CP conserving spectrum. This means that in calculations of observables, such as the relic density or rare decay branching ratios, the dominant effect comes from the new light scalar introduced by SCPV in our model.

We already discussed that for B physics constraints the effect of small CP-violating phases is negligible. We additionally find that the appearance of  $h_S$  has very little effect since it doesn't appear in the calculations of  $\text{BR}(B \rightarrow X_s \gamma)$ ,  $\text{BR}(B^+ \rightarrow \tau^+ \nu_\tau)$ , and  $\text{BR}(B_s \rightarrow \mu^+ \mu^-)$  until two loop order. The charged Higgses contribute already at lower order but their masses change continuously with the CP phases and thus the effect of CP violation remains limited in the regime of small CP phases. However, in the case of the relic density there are new, possibly dominant, annihilation channels that open up with the appearance of  $h_S$  depending on what kind of LSP we have.

Figures 1 and 3 show the leading coefficients for two classes of direct annihilation channels, i.e., those with  $f\bar{f}$ ,  $f \in [q, l, \nu]$ , and those with  $h_S h_S$  final states in the case of a neutralino or a sneutrino LSP, respectively. We show neither the diagrams for vector boson final states nor for the various co-annihilation channels; the coefficients are all sub leading or the same as for the  $f\bar{f}$  diagrams. In the numerical calculations we naturally take all these channels into account. As we can show, this rough approximation provides a good understanding of the parametric dependence of the relic density. We have abbreviated the typical electroweak coupling  $\frac{e}{2s_W c_W} \equiv C \simeq 0.37$ .



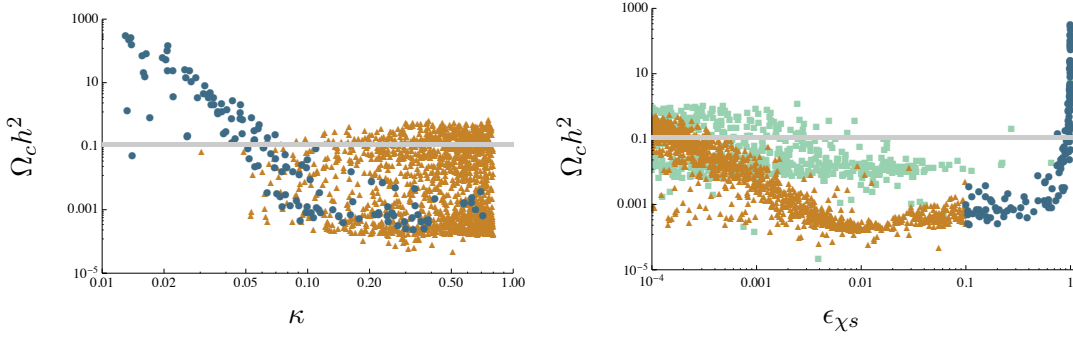
**Figure 1.** Tree level pair annihilation channels for the neutralino into  $f\bar{f}/h_S h_S$ . Leading coefficients for the doublet (d) and singlet (s) component of the neutralino are given. The addition of a light singlet scalar to the spectrum opens additional channels.

Fig. 1 shows the pair annihilation channels in the case of a neutralino LSP. We have separated the leading coefficients for the case of a pure singlino as “singlet” and group the couplings to all the other gauge eigenstates under “doublet”. We see that for the doublet component of the neutralino the dominant contributions are  $\sim C^2$  with most of the new  $h_S$  final states suppressed by  $\epsilon_{sd}$ .

For the singlet component of the neutralino the story is different. The unsuppressed  $\sim \lambda_N, \lambda_N^2$  channels for the  $f\bar{f}$  final states are available only if the right-handed neutrino is lighter than the LSP. Even then,  $m_{\nu_R}$  depends on  $\lambda_N$  directly so having  $m_{\nu_R}$  small may also significantly suppress these channels if, e.g.,  $\langle S \rangle$  is large. The channels for  $h_S$  final states on the other hand contain unsuppressed  $\kappa^2$  dependence. However,  $\kappa$  also controls

the neutralino mixing in a way that for small values of  $\kappa$  the LSP becomes highly singlino dominated. In that case, the only available annihilation channels are those now suppressed by the smallness of  $\kappa$ , which leads to a larger relic density.

These effects are shown in Fig. 2. In the left plot we can see that for small values of  $\kappa \lesssim 0.05$  none of the neutralinos have an appreciable doublet component and also that the relic density for singlino dominated LSPs is controlled by  $\kappa$ . In the right plot we see how with a growing singlino component the presence of the new  $h_S$  final state channels significantly decrease the relic density compared to the CP-conserving scenario beginning at  $\epsilon_{\chi s} \gtrsim 0.001$ . We also see that once only the singlino channels are available the relic density can again become very large due to suppression by  $\kappa$ .



**Figure 2.** Left: The relic density against the trilinear coupling  $\kappa$  for neutralino LSPs. Right: The relic density against the singlino component of the neutralino LSP. Points with (blue circles) and without (orange triangles) significant singlino component. Green boxes depict points from the CP-conserving data set. The grey band indicates the the current WMAP limits on the relic density.

Fig. 3 shows the pair annihilation channels for the sneutrino LSP. In the case of a left-handed sneutrino the channels decaying into  $h_S h_S$  are suppressed by additional factors of  $C^2$  and/or  $\epsilon_{sd}$ . It is known that the left-handed sneutrino is a poor LSP candidate if one wants to saturate the dark matter relic density limit [60]. This is caused by the fact that the dominant  $\sim C^2$  weak decay channel is always present for the left-handed sneutrino.

In the case of a right-handed sneutrino Fig. 3 shows that the  $h_S h_S$  channels are all of the same order as the  $f \bar{f}$  channels and collectively depend to leading order on  $\lambda_N$  or  $\lambda_N^2$ . Thus, it is expected that the relic density will be lower when compared to the CP-conserving case. The left plot in Fig. 4 shows how the relic density for right-handed sneutrinos depends strongly on  $\lambda_N$ , while the relic density for left-handed sneutrinos stays almost a constant. The right plot in Fig. 4 shows the drop of the relic density for the CP-violating case for right-handed sneutrino LSPs when compared to the CP-conserving data. Although much of the set overlaps there is a clear systematic drop in the mean relic density for the CP-violating set.

In Fig. 5 all of the aforementioned effects are shown in unison. In the plot on the left the fixed gaugino mass  $M_1 = 300$  GeV causes the neutralino relic density to spike at  $m_{LSP} = M_1$  due to the small bino annihilation process cross section. We also see that for

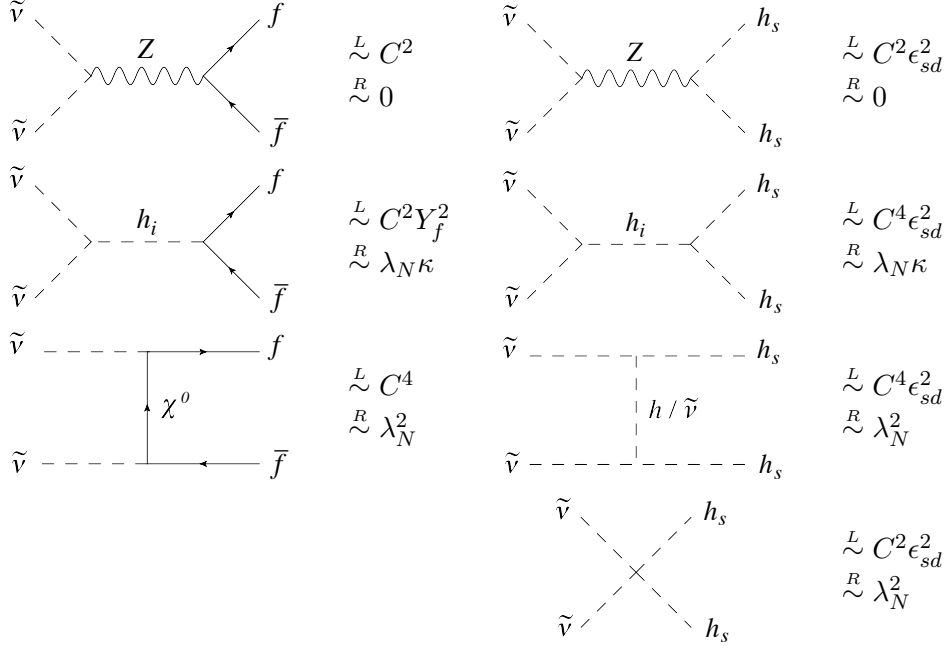


**Figure 3.** Tree level pair annihilation channels for the sneutrino into  $f\bar{f}/h_S h_S$ . Leading coefficients for the left-handed (L) and right-handed (R) case are given. In the left-handed case the addition of a light singlet to the spectrum opens up new channels but they are all suppressed by additional factors of  $C^2$  or  $\epsilon_{sd}^2$  when compared to the originally dominant weak decay channel. In the right-handed case the new  $h_S$  final state channels are of the same order as the other decay channels.

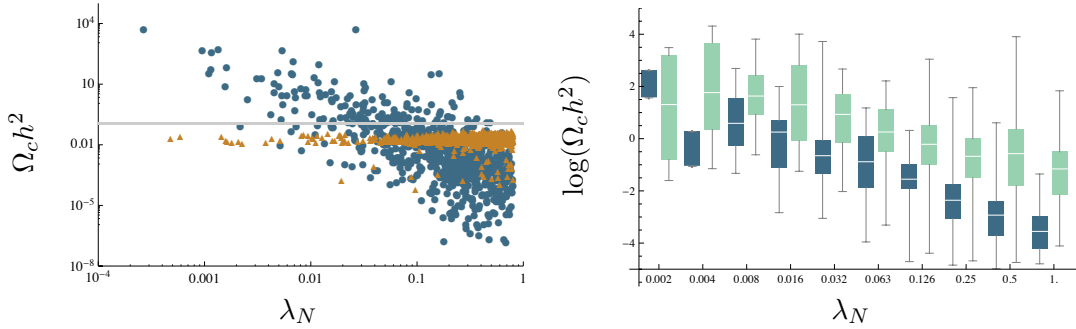


**Figure 4.** Left: The relic density against the trilinear coupling  $\lambda_N$  for right-handed (blue circles) and left-handed (orange triangles) sneutrino LSPs. The grey band indicates the current WMAP limits on the relic density. Right: A box-and-whisker diagram of the relic density against the trilinear coupling  $\lambda_N$  comparing the distribution of right-handed sneutrino LSPs in the CP-conserving (light green) and CP-violating (blue) cases. Boxes are the 25 - 75 percentile range and whiskers denote the complete range of the data.

other values of  $m_{LSP}$  the neutralino has to be singlino dominated (yellow dot) if we want to saturate the relic density limit and how in the case of CP violation the relic density is significantly reduced compared to the CP conserving case. In the right plot we see

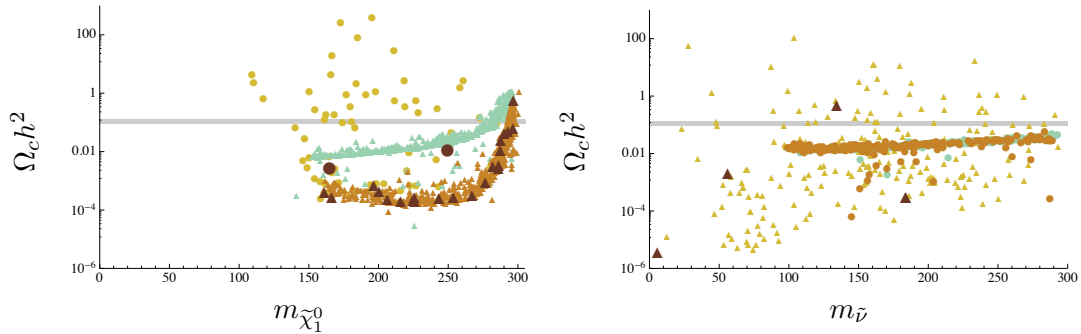


**Figure 5.** The relic density against the LSP mass. Left: for neutralino LSPs in the CP-conserving (light green triangle), CP-violating doublet dominated (orange triangle) and CP-violating significant singlino admixture, i.e.  $\epsilon_{\chi s} > 0.1$ , (yellow dot) cases. Right: for sneutrino LSPs in the CP-violating left-handed (orange dot) and CP-violating right-handed (yellow triangle) case. The CP-conserving left-handed (light green dot) set overlaps completely with the CP-violating counterpart. In both plots all points satisfy PDG constraints on the mass spectrum and vacuum stability, large brown triangles or circles indicate points that pass all of the other experimental constraints we impose. The grey band indicates the current WMAP limits on the relic density.

that left-handed sneutrino LSPs are poor candidates for saturating the relic density limit regardless of CP violation, whereas for right-handed sneutrinos this is not a problem. The scattered very low relic density points for the left-handed sneutrinos are due to the presence of efficient slepton co-annihilations. Both plots also show how few points pass all of the experimental constraints we impose. We find that the most restrictive constraint is the electron EDM, e.g., in Fig. 5 removing all other CP, B physics, and rare decay constraints only yields a single additional “allowed” point.

In general we find that for constrained phases the effect on the relic density from variations in the spectrum of the model is much smaller than the effect introduced by the appearance of a light singlet scalar providing new annihilation channels for the LSP. Depending on the LSP and its composition these channels are governed by the Lagrangian parameters  $\kappa$  and  $\lambda_N$ .

## 5 Direct dark matter searches

There are currently several ongoing searches of weakly interacting massive particles (WIMPs) in direct detection experiments. The goal of the experiments is to measure the WIMP–nucleus interaction in the detector material. WIMPs scatter when they interact with nuclei, and the recoil energy can then be measured. As yet, the XENON100 experiment puts the tightest limits on the WIMP-nucleon scattering cross section [61]. To compare the calculated proton/neutron cross sections with the experimental limits, we use a normalized cross section for a point-like nucleus [62]:

$$\sigma_{\text{SI}} = \frac{(Z\sqrt{\sigma_p} + (A - Z)\sqrt{\sigma_n})^2}{A^2}, \quad (5.1)$$

$Z$  and  $A$  being the atomic and mass number of the target element<sup>1</sup> and  $\sigma_{n,p}$  the spin-independent cross-sections for neutron and proton target, respectively. Because there are large uncertainties in the local density of dark matter and in the nuclear matrix elements that enter the computation of  $\sigma_{SI}$  [63, 64], the direct detection limits are only indicative.

Fig. 6 shows the LSP mass versus the spin independent cross section for a set of CP-violating points, as well as the XENON100 limit. We see that the XENON100 limit actually

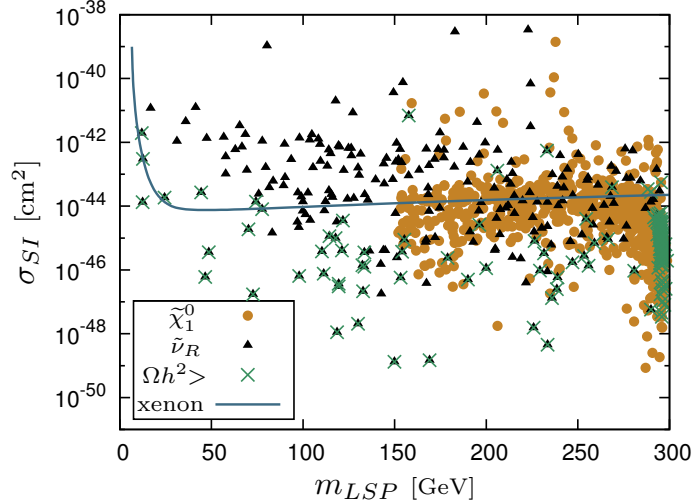


**Figure 6.** Spin-independent WIMP–nucleon cross section for CPV points. Points with triangular shape (black) have the right-handed sneutrino as an LSP, while the dots (orange) have neutralino LSP. The (green) cross above a point corresponds to a relic density above the WMAP upper limit, hence an excluded point. The solid line represents the XENON100 experimental limit.

serves as a constraint, since a relatively large portion of the parameter points are ruled out by the direct detection search. A roughly equal number of points are still allowed by the XENON100 limit. The WMAP upper limit constraint removes most of the sneutrino LSP points allowed by the XENON100 limit. However, some points still evade both dark matter constraints. A large number of neutralino LSP points are still allowed in the low neutralino mass region. In ref. [65] it was found that in the CP-conserving NMSSM the direct detection limits for the neutralino LSP still allow a large number of points with low fine tuning, especially for a large  $\lambda$  parameter.

## 6 Signatures at the colliders

In this section we focus on the possible signals from the supersymmetric particle spectrum realized by the model respecting all relevant low energy constraints and generating an acceptable amount of relic density. Notwithstanding the fact that we have already restricted the parameter space of the model significantly by various constraints, recent observation of a  $\sim 125 - 126$  GeV Higgs like boson at LHC by both the CMS [66] and ATLAS [67] Collaborations further helps in narrowing down the allowed sparticle spectrum.

<sup>1</sup>For Xenon:  $A = 131$ ,  $Z = 54$ .

As discussed in Sec. 4 in the model used here with SCPV a light scalar state  $h_1 \equiv h_S$  exists and thus the branching ratio of the decay of the  $\sim 125$  GeV Higgs,  $h_2$ , into a pair  $h_S$  is of particular interest. A limit on  $\text{BR}(h_2 \rightarrow h_S h_S)$  could be useful in further constraining this type model. We find that *a priori* requiring  $m_{h_S} > m_{h_2}/2$  is problematic since a larger mass for the singlet type Higgs implies larger CP violation and thus the limits on the EDMs exclude these points. Instead we extract the  $h h h$  coupling as

$$C_{ijk}^{hhh} = i \sum_{r,s,t}^{6,6,6} \mathcal{O}_{ir} \mathcal{O}_{js} \mathcal{O}_{kt} \frac{\delta}{\delta \phi_r} \frac{\delta}{\delta \phi_s} \frac{\delta}{\delta \phi_t} \mathcal{L}_{int}|_{\text{vev}}, \quad (6.1)$$

$$\phi \in \{\text{Re}H_1^0, \text{Re}H_2^0, \text{Re}S, \text{Im}H_1^0, \text{Im}H_2^0, \text{Im}S\} \quad (6.2)$$

with  $\mathcal{O}$  the Higgs mixing matrix and require  $|C_{211}^{hhh}| < 1\text{GeV}$ . From the points that clear this limit we have selected a few which also clear the EDM, B-physics, and rare decay constraints and are favored by relic density and analyze their signal at LHC. We have listed the benchmark points (BP) in Table 2. Note that LHC has already put some strong limits on the squark and gluino masses [68, 69], albeit these constraints are model dependent and also depend on the way the heavy particles decay. However, for our analysis, we have made a consistent choice of parameters where the strongly interacting sector of the sparticle spectrum remains above a TeV and is, therefore, unconstrained from LHC data. This implies that our analysis will focus on the weakly interacting sector of the spectrum *viz.*, sleptons, gauginos/higgsinos and the Higgs.

Our choice for parameter points leads to a right-handed sneutrino LSP or a neutralino LSP. For BP6 and BP7 the LSP comes out to be a right-handed sneutrino with a mass of  $\sim 6$  GeV and  $\sim 184$  GeV, respectively. All the other benchmark points have a neutralino as an LSP. We focus on each benchmark point individually and highlight the most likely signals for the different parameter choices at LHC in our model.

	BP1	BP2	BP3	BP4	BP5	BP6	BP7
$\tan\beta$	45.7	12.4	33.9	26.9	30.1	43.5	44.9
$\lambda$	0.114	0.355	0.363	0.347	0.430	0.259	0.341
$\kappa$	0.038	0.63	0.231	0.294	0.357	0.174	0.292
$v_S$ (GeV)	4277.2	1160.2	964.8	914.8	487.5	1881.9	816.7
$\lambda_N$	0.721	0.008	0.032	0.498	0.269	0.035	0.750
$A_{\lambda_N}$ (GeV)	337.0	25.2	-668.9	319.7	365.3	-135.5	-975.5
$M_N$ (GeV)	447.7	449.8	494.7	401.1	341.5	207.6	135.7
$M_{L,E}$ (GeV)	307.1	419.5	432.0	431.9	472.7	320.3	377.0
$\delta_S$	3.228	0.156	3.142	3.203	3.213	3.199	3.173
$\delta_2$	0.111	0.034	0.010	0.249	3.037	0.142	0.173
$\xi$ (GeV)	118.1	-991.3	522.9	318.9	253.0	109.8	300.6
LSP-type	$\chi_0$	$\chi_0$	$\chi_0$	$\chi_0$	$\chi_0$	$\tilde{\nu}_R$	$\tilde{\nu}_R$
$m_{LSP}$ (GeV)	296.3	290.9	286.3	276.7	194.6	5.7	183.7
$\Omega_c h^2$	0.062	0.098	$8.3 \cdot 10^{-3}$	$8.3 \cdot 10^{-4}$	$6.5 \cdot 10^{-4}$	$3.3 \cdot 10^{-6}$	$2.9 \cdot 10^{-4}$

**Table 2.** Benchmark points for studying the signals of the supersymmetric particles at LHC. Note that  $\mu = \lambda v_S$  and other parameters are the same as shown in Table 1.

### • BP1

This point gives a neutralino LSP with mass  $\sim 296$  GeV while the lightest sneutrino is nearly degenerate at  $\sim 300$  GeV. The chargino  $\chi_1^+$  is much heavier (470 GeV) than the second neutralino  $\chi_2^0$  (322 GeV). Although this point is allowed by all experimental data it does not give any significant cross sections at LHC in any channel. The chargino pair production which is the largest is about 8 fb at LHC with  $\sqrt{s} = 14$  TeV. The dominant decay for the chargino is to charged leptons and lighter sneutrinos which then decay invisibly. So the final state which could be observed at LHC is  $\ell_i^+ \ell_j^- \cancel{E}_T$  which would require substantial luminosity to separate it from the large SM background coming from the  $W^+W^-$  production. The point also gives a very light scalar of  $\sim 2.7$  GeV which is dominantly singlet with very suppressed couplings to all SM particles, such that it is not constrained by any experimental data.

### • BP2

For this point we have a relatively small  $\tan\beta$  and  $\lambda_N$  as compared to all other points. The LSP is the lightest neutralino which has a mass of  $\sim 291$  GeV. The small value of  $\lambda_N$  leads to a very light right-handed neutrino of mass  $\sim 19$  GeV. This state has a very small mixing with the left-handed neutrino and thus is not constrained by the measured  $Z$  width or other low energy data. The strongest signal for this point at LHC is through the production of first chargino and second neutralino ( $\chi_1^+ \chi_2^0$ ) whose mass is about 400 GeV with a cross section of  $\sim 5$  fb for the current run at LHC with  $\sqrt{s} = 8$  TeV while the next significant production cross section is for the pair production of charginos ( $\chi_1^+ \chi_1^-$ ) with a cross section of  $\sim 4$  fb. All other production modes are suppressed. The cross sections are increased by a factor of  $\sim 3 - 4$  at LHC with  $\sqrt{s} = 14$  TeV while other modes also become accessible with high luminosity.



However, we note that the mass difference of these states with the LSP is only about 100 GeV. Both the  $\chi_1^+$  and  $\chi_2^0$  decay to the LSP and a weak gauge boson with 100% branching probability. Thus the pair production of charginos will lead to a final state of  $W^+W^- \cancel{E}_T$  where both  $W$ 's will have small transverse momenta. The  $\chi_1^+\chi_2^0$  production leads to final states with  $W^+Z \cancel{E}_T$  with no suppression in branching ratios. This leads to interesting signal of a Z peak, an associated charged lepton and large missing energy. The SM background will be mostly from  $WZ$  and triple gauge boson production where the large  $WZ$  production can be suppressed by demanding large  $\cancel{E}_T$ .

- **BP3**

This point gives a neutralino LSP with a mass of  $\sim 286$  GeV with next lightest supersymmetric particles being  $\chi_2^0$  (338 GeV) and  $\chi_1^+$  (341 GeV). This point also gives us a light right-handed neutrino with mass 61 GeV and an ultralight scalar with mass 300 MeV. The largest production cross section in this case is again  $\chi_1^+\chi_1^-$  and  $\chi_1^+\chi_2^0$  but the  $\chi_1^+$  decays via off-shell weak gauge boson ( $W^+$ ) and off-shell sleptons/sneutrinos leading to final state particles with small transverse momenta. The  $\chi_2^0$  decays to an ultralight singlet scalar and the LSP with 100% probability. The signal production cross sections are about  $\sim 7.5$  fb and  $\sim 3$  fb, respectively, at LHC with  $\sqrt{s} = 8$  TeV, and a factor  $\sim 3-4$  larger at LHC with  $\sqrt{s} = 14$  TeV. As the final decay products do not carry large transverse momenta, isolating the signal from the background will be very challenging.

- **BP4**

This point has a very similar spectrum to BP3 except for a much heavier right-handed neutrino with a mass of  $\sim 910$  GeV as  $\lambda_N$  is much larger. The lightest scalar is the dominantly singlet component of the Higgs with mass  $\sim 17$  GeV. The neutralino LSP has a mass of  $\sim 277$  GeV. The next to lightest supersymmetric particle (NLSP) is the  $\chi_1^+$  (311 GeV) while  $\chi_2^0$  (316 GeV) also is close and nearly degenerate. The mass difference again forces the decay similar to that for BP3 with final states with small transverse momenta. The largest cross section in this case is for the pair production of charginos ( $\chi_1^+\chi_1^-$ ) which is about 13 fb at LHC with  $\sqrt{s} = 8$  TeV which increases to  $\sim 40$  fb for  $\sqrt{s} = 14$  TeV.

- **BP5**

This point corresponds to a much lighter supersymmetric spectrum with a neutralino LSP of mass  $\sim 195$  GeV. The NLSP is  $\chi_2^0$  (199 GeV) with  $\chi_1^+$  (204.5 GeV) the next lightest. It also has a 262 GeV right-handed neutrino. The light spectrum leads to much larger production cross sections, and the dominant production channels in this case are  $\chi_1^+\chi_1^-$ ,  $\chi_1^+\chi_1^0$  and  $\chi_1^+\chi_2^0$  with production cross sections of around 74 fb, 86 fb and 82 fb, respectively, at LHC with  $\sqrt{s} = 8$  TeV. However, the mass difference of  $\chi_1^+$  and  $\chi_2^0$  with  $\chi_1^0$  is less than 10 GeV, and thus the transverse energy of the decay products is small. It would be quite difficult to trigger on such soft leptons

and jets that result from the 3-body decays of  $\chi_1^+$  and  $\chi_2^0$ . A detailed analysis would be required to isolate signals which would be relevant to highlight for LHC searches.

- **BP6**

Unlike the other points, we get a right sneutrino LSP for this parameter choice with a mass of  $\sim 6$  GeV. Pair production of the LSP has the largest cross section but will pass through the detector undetected. The other significant cross sections ( $\chi_1^+ \chi_1^-$ ,  $\chi_1^+ \chi_2^0$ ) are relevant only at LHC with  $\sqrt{s} = 14$  TeV with production cross sections of less than 8 fb. The decay of the  $\chi_1^+$  and  $\chi_2^0$  is however different from that of BP2 with suppressed probabilities in similar channels and therefore the signal gets suppressed further. Much like BP1 we get a light scalar with a mass of  $\sim 2.5$  GeV. We also get a light right-handed neutrino of mass 130 GeV which can lead to interesting signals if there is significant mixing with the left-handed neutrinos.

- **BP7**

Our final benchmark point gives us a right sneutrino LSP of mass  $\sim 184$  GeV. This point also gives a light scalar Higgs of mass  $\sim 8.4$  GeV in the mass spectrum. The  $\chi_1^0$  (254 GeV) is the NLSP while the right-handed neutrino mass is above 1 TeV. The largest production cross section in this case is for  $\chi_1^+ \chi_1^-$  where the chargino mass is  $\sim 273$  GeV, which at LHC with  $\sqrt{s} = 8$  TeV is about 22 fb and jumps up to  $\sim 65$  fb for  $\sqrt{s} = 14$  TeV. The chargino decays to a  $\tau$  and LSP with 60% branching probability while it decays 20% of the time to electron/muon and LSP. This leads to final states of two charged leptons with large missing energy. Other relevant channels are from production of  $\chi_1^0 \chi_2^0$ ,  $\chi_1^+ \chi_1^0$  and  $\chi_1^+ \chi_2^0$  where the  $\chi_1^0$  decays invisibly while the  $\chi_2^0$  decays to the light scalar Higgs and  $\chi_1^0$  with 100% probability.

Although we discuss some possible signals at LHC for our model with different choices of the parameter space a more detailed analysis of both signal and background is needed which we leave for future work. The CP-violating effects due to non-zero phases can affect several observables reconstructed from the cascade decays of the charginos, neutralinos or the scalars in the model and have been highlighted in various studies [70–73] and we aim to apply these studies in our future analysis of the model at LHC in our next publication [74].

## 7 Summary and discussion

We have studied the viability of the right-handed sneutrino and neutralino dark matter in the NMSSM, and the effect of CP violation on the dark matter relic density and the direct detection potential. The studied model contains, in addition to the MSSM fields, two singlet superfields and interaction terms. This extends the Higgs sector, adds the right-handed neutrino field to the model, and allows the right-handed sneutrino to become a thermally produced dark matter candidate. We took into account the  $\text{BR}(B \rightarrow X_s \gamma)$ ,  $\text{BR}(B^+ \rightarrow \tau^+ \nu_\tau)$ , and  $\text{BR}(B_s \rightarrow \mu^+ \mu^-)$  bounds, the discovery of the Higgs and sparticle

searches, and constrained the model parameters by calculating the dark matter relic density, including co-annihilations. We calculated also the direct detection rates for the nucleon–DM spin-independent cross section, and compared that to the XENON100 limit. We have found that for constrained CP-violating phases the effect on the relic density from variations in the spectrum of the model is much smaller than the effect introduced by the appearance of a light singlet scalar providing new annihilation channels for the LSP. In particular for neutralinos and right-handed sneutrinos these new channels lower the relic density. In some cases, the left-handed sneutrinos co-annihilate very efficiently with other sleptons resulting in very low relic density. The spin-independent cross section can be used to constrain the models with a light sneutrino LSP, as for these models the direct detection limit tends to be complementary to the relic density constraint. The neutralino dark matter, however, remains rather unconstrained by the direct detection limits. We have also used our analysis to identify a set of benchmark points which satisfy all constraints and favor DM data. We have used these benchmark points to highlight the most important signals for the model that can be observed at the current and future run of the LHC.

## 8 Acknowledgments

KH, LL, and TR acknowledge support from the Academy of Finland (Project No. 137960). The work of JL is supported by the Foundation for Fundamental Research of Matter (FOM), program 104 “Theoretical Particle Physics in the Era of the LHC”. LL thanks Magnus Ehrnrooth Foundation for financial support. SKR is supported in part by the United States Department of Energy, Grant Number DE-FG02-04ER41306.

## References

- [1] **WMAP** Collaboration, E. Komatsu *et. al.*, *Seven-Year Wilkinson Microwave Anisotropy Probe (WMAP) Observations: Cosmological Interpretation*, *Astrophys.J.Suppl.* **192** (2011) 18, [[arXiv:1001.4538](#)].
- [2] A. Salam and J. A. Strathdee, *Supersymmetry and fermion number conservation*, *Nucl. Phys.* **B87** (1975) 85.
- [3] P. Fayet, *Supergauge Invariant Extension of the Higgs Mechanism and a Model for the electron and Its Neutrino*, *Nucl.Phys.* **B90** (1975) 104–124.
- [4] G. R. Farrar and P. Fayet, *Phenomenology of the production, decay, and detection of new hadronic states associated with supersymmetry*, *Phys. Lett.* **B76** (1978) 575–579.
- [5] S. Dimopoulos, S. Raby, and F. Wilczek, *Proton decay in supersymmetric models*, *Phys. Lett.* **B112** (1982) 133.
- [6] G. R. Farrar and S. Weinberg, *Supersymmetry at ordinary energies. 2. R invariance, Goldstone bosons, and gauge fermion masses*, *Phys. Rev.* **D27** (1983) 2732.
- [7] D. O. Caldwell, R. Eisberg, D. Grumm, M. S. Witherell, B. Sadoulet, *et. al.*, *Laboratory Limits on Galactic Cold Dark Matter*, *Phys.Rev.Lett.* **61** (1988) 510.
- [8] D. O. Caldwell, B. Magnusson, M. S. Witherell, A. Da Silva, B. Sadoulet, *et. al.*, *Searching for the cosmion by scattering in Si detectors*, *Phys.Rev.Lett.* **65** (1990) 1305–1308.

- [9] D. Reusser, M. Treichel, F. Boehm, C. Brogini, P. Fisher, *et. al.*, *Limits on cold dark matter from the Gotthard Ge experiment*, *Phys.Lett.* **B255** (1991) 143–145.
- [10] **KAMIOKANDE** Collaboration, M. Mori *et. al.*, *Search for neutralino dark matter in Kamiokande*, *Phys.Rev.* **D48** (1993) 5505–5518.
- [11] T. Asaka, K. Ishiwata, and T. Moroi, *Right-handed sneutrino as cold dark matter*, *Phys. Rev.* **D73** (2006) 051301, [[hep-ph/0512118](#)].
- [12] T. Asaka, K. Ishiwata, and T. Moroi, *Right-handed sneutrino as cold dark matter of the universe*, *Phys. Rev.* **D75** (2007) 065001, [[hep-ph/0612211](#)].
- [13] M. Dugan, B. Grinstein, and L. J. Hall, *CP Violation in the Minimal N=1 Supergravity Theory*, *Nucl.Phys.* **B255** (1985) 413.
- [14] M. Gavela, P. Hernandez, J. Orloff, O. Pene, and C. Quimbay, *Standard model CP violation and baryon asymmetry. Part 2: Finite temperature*, *Nucl.Phys.* **B430** (1994) 382–426, [[hep-ph/9406289](#)].
- [15] J. R. Ellis, S. Ferrara, and D. V. Nanopoulos, *CP Violation and Supersymmetry*, *Phys.Lett.* **B114** (1982) 231.
- [16] J. Polchinski and M. B. Wise, *The Electric Dipole Moment of the Neutron in Low-Energy Supergravity*, *Phys.Lett.* **B125** (1983) 393.
- [17] T. Lee, *A Theory of Spontaneous T Violation*, *Phys.Rev.* **D8** (1973) 1226–1239.
- [18] G. Hiller, K. Huitu, T. Ruppell, and J. Laamanen, *A Large Muon Electric Dipole Moment from Flavor?*, *Phys.Rev.* **D82** (2010) 093015, [[arXiv:1008.5091](#)].
- [19] M. Masip and A. Rasin, *Minimal supersymmetric scenarios for spontaneous CP violation*, *Phys.Rev.* **D58** (1998) 035007, [[hep-ph/9803271](#)].
- [20] R. Mohapatra and C. Nishi, *Absence of Spontaneous CP violation in Multi-Higgs Doublet Extension of MSSM*, *Phys.Rev.* **D84** (2011) 095023, [[arXiv:1108.1769](#)].
- [21] J. R. Ellis, J. Gunion, H. E. Haber, L. Roszkowski, and F. Zwirner, *Higgs Bosons in a Nonminimal Supersymmetric Model*, *Phys.Rev.* **D39** (1989) 844.
- [22] M. Drees, *Supersymmetric Models with Extended Higgs Sector*, *Int.J.Mod.Phys.* **A4** (1989) 3635.
- [23] U. Ellwanger, C. Hugonie, and A. M. Teixeira, *The Next-to-Minimal Supersymmetric Standard Model*, *Phys.Rept.* **496** (2010) 1–77, [[arXiv:0910.1785](#)].
- [24] J. E. Kim and H. P. Nilles, *The mu Problem and the Strong CP Problem*, *Phys.Lett.* **B138** (1984) 150.
- [25] J. Goldstone, A. Salam, and S. Weinberg, *Broken Symmetries*, *Phys.Rev.* **127** (1962) 965–970.
- [26] D. G. Cerdeno and O. Seto, *Right-handed sneutrino dark matter in the NMSSM*, *JCAP* **0908** (2009) 032, [[arXiv:0903.4677](#)].
- [27] D. G. Cerdeno, J.-H. Huh, M. Peiro, and O. Seto, *Very light right-handed sneutrino dark matter in the NMSSM*, *JCAP* **1111** (2011) 027, [[arXiv:1108.0978](#)].
- [28] J.-J. Cao, K.-i. Hikasa, W. Wang, J. M. Yang, K.-i. Hikasa, *et. al.*, *Light dark matter in NMSSM and implication on Higgs phenomenology*, *Phys.Lett.* **B703** (2011) 292–297, [[arXiv:1104.1754](#)].

- [29] D. A. Vasquez, G. Belanger, C. Boehm, J. Da Silva, P. Richardson, *et. al.*, *The 125 GeV Higgs in the NMSSM in light of LHC results and astrophysics constraints*, *Phys.Rev.* **D86** (2012) 035023, [[arXiv:1203.3446](#)].
- [30] M. Frank, K. Huitu, and T. Ruppell, *Spontaneous CP and R parity breaking in supersymmetry*, [hep-ph/0508056](#).
- [31] C. Hugonie, J. C. Romao, and A. M. Teixeira, *Spontaneous CP violation in nonminimal supersymmetric models*, *JHEP* **0306** (2003) 020, [[hep-ph/0304116](#)].
- [32] A. Abada, G. Bhattacharyya, D. Das, and C. Weiland, *A possible connection between neutrino mass generation and the lightness of a NMSSM pseudoscalar*, *Phys.Lett.* **B700** (2011) 351–355, [[arXiv:1011.5037](#)].
- [33] D. Das and S. Roy, *One-loop contribution to the neutrino mass matrix in NMSSM with right-handed neutrinos and tri-bimaximal mixing*, *Phys.Rev.* **D82** (2010) 035002, [[arXiv:1003.4381](#)].
- [34] Z. Kang, J. Li, T. Li, T. Liu, and J. Yang, *Asymmetric Sneutrino Dark Matter in the NMSSM with Minimal Inverse Seesaw*, [arXiv:1102.5644](#).
- [35] A. Semenov, *LanHEP - a package for automatic generation of Feynman rules from the Lagrangian. Updated version 3.1*, [arXiv:1005.1909](#).
- [36] G. Belanger, F. Boudjema, A. Pukhov, and A. Semenov, *MicrOMEGAs 2.0: A Program to calculate the relic density of dark matter in a generic model*, *Comput.Phys.Commun.* **176** (2007) 367–382, [[hep-ph/0607059](#)].
- [37] B. Garbow, *Eispack - a package of matrix eigensystem routines*, *Comput.Phys.Commun.* **7** (1974) 179–184.
- [38] U. Ellwanger and C. Hugonie, *NMHDECAY 2.0: An Updated program for sparticle masses, Higgs masses, couplings and decay widths in the NMSSM*, *Comput.Phys.Commun.* **175** (2006) 290–303, [[hep-ph/0508022](#)].
- [39] U. Ellwanger and C. Hugonie, *NMSPEC: A Fortran code for the sparticle and Higgs masses in the NMSSM with GUT scale boundary conditions*, *Comput.Phys.Commun.* **177** (2007) 399–407, [[hep-ph/0612134](#)].
- [40] **Particle Data Group** Collaboration, K. Nakamura *et. al.*, *Review of particle physics*, *J.Phys.G* **G37** (2010) 075021.
- [41] **ALEPH, DELPHI, L3, OPAL, LEP WG for Higgs Boson Searches** Collaboration, S. Schael *et. al.*, *Search for neutral MSSM Higgs bosons at LEP*, *Eur.Phys.J.* **C47** (2006) 547–587, [[hep-ex/0602042](#)].
- [42] ATLAS Collaboration, *Combined search for the Standard Model Higgs boson using up to 4.9 fb<sup>-1</sup> of pp collision data at  $\sqrt{s} = 7$  TeV with the ATLAS detector at the LHC*, [arXiv:1202.1408](#).
- [43] **CMS** Collaboration, S. Chatrchyan *et. al.*, *Combined results of searches for the standard model Higgs boson in pp collisions at  $\sqrt{s} = 7$  TeV*, [arXiv:1202.1488](#).
- [44] U. Ellwanger, *A Higgs boson near 125 GeV with enhanced di-photon signal in the NMSSM*, [arXiv:1112.3548](#).
- [45] J. F. Gunion, Y. Jiang, and S. Kraml, *The Constrained NMSSM and Higgs near 125 GeV*, [arXiv:1201.0982](#).

- [46] S. King, M. Muhlleitner, and R. Nevzorov, *NMSSM Higgs Benchmarks Near 125 GeV*, [arXiv:1201.2671](#).
- [47] D. A. Vasquez, G. Belanger, C. Boehm, J. Da Silva, P. Richardson, *et. al.*, *The 125 GeV Higgs in the NMSSM in light of LHC results and astrophysics constraints*, [arXiv:1203.3446](#).
- [48] **Particle Data Group** Collaboration, J. Beringer *et. al.*, *Review of Particle Physics (RPP)*, *Phys.Rev.* **D86** (2012) 010001.
- [49] G. Hiller, *B physics signals of the lightest CP odd Higgs in the NMSSM at large tan beta*, *Phys.Rev.* **D70** (2004) 034018, [[hep-ph/0404220](#)].
- [50] F. Domingo and U. Ellwanger, *Updated Constraints from B Physics on the MSSM and the NMSSM*, *JHEP* **0712** (2007) 090, [[arXiv:0710.3714](#)].
- [51] M. Misiak, H. Asatrian, K. Bieri, M. Czakon, A. Czarnecki, *et. al.*, *Estimate of  $B(\text{anti-}B \rightarrow X(s) \gamma)$  at  $O(\alpha(s)^2)$* , *Phys.Rev.Lett.* **98** (2007) 022002, [[hep-ph/0609232](#)].
- [52] J. R. Ellis, S. Heinemeyer, K. A. Olive, A. M. Weber, and G. Weiglein, *The Supersymmetric Parameter Space in Light of  $B^-$  physics Observables and Electroweak Precision Data*, *JHEP* **08** (2007) 083, [[arXiv:0706.0652](#)].
- [53] **Heavy Flavor Averaging Group** Collaboration, D. Asner *et. al.*, *Averages of b-hadron, c-hadron, and tau-lepton Properties*, [arXiv:1010.1589](#).
- [54] K. Huitu, L. Leinonen, and J. Laamanen, *Stop as a next-to-lightest supersymmetric particle in constrained MSSM*, *Phys.Rev.* **D84** (2011) 075021, [[arXiv:1107.2128](#)].
- [55] G. Isidori and P. Paradisi, *Hints of large tan(beta) in flavour physics*, *Phys.Lett.* **B639** (2006) 499–507, [[hep-ph/0605012](#)].
- [56] B. Bhattacharjee, A. Dighe, D. Ghosh, and S. Raychaudhuri, *Do new data on  $[B+ \rightarrow \tau + \nu \tau]$  decays point to an early discovery of supersymmetry at the LHC?*, *Phys.Rev.* **D83** (2011) 094026, [[arXiv:1012.1052](#)].
- [57] **LHCb collaboration** Collaboration, R. Aaij *et. al.*, *Strong constraints on the rare decays  $B_s \rightarrow \mu^+ \mu^-$  and  $B^0 \rightarrow \mu^+ \mu^-$* , *Phys.Rev.Lett.* **108** (2012) 231801, [[arXiv:1203.4493](#)].
- [58] N. Baro, F. Boudjema, and A. Semenov, *Full one-loop corrections to the relic density in the MSSM: A few examples*, *Phys. Lett.* **B660** (2008) 550–560, [[arXiv:0710.1821](#)].
- [59] H. Georgi and A. Pais, *CP-Violation as a Quantum Effect*, *Phys.Rev.* **D10** (1974) 1246.
- [60] T. Falk, K. A. Olive, and M. Srednicki, *Heavy sneutrinos as dark matter*, *Phys.Lett.* **B339** (1994) 248–251, [[hep-ph/9409270](#)].
- [61] **XENON100** Collaboration, E. Aprile *et. al.*, *The XENON100 Dark Matter Experiment*, *Astropart.Phys.* **35** (2012) 573–590, [[arXiv:1107.2155](#)].
- [62] G. Belanger, M. Kakizaki, E. Park, S. Kraml, and A. Pukhov, *Light mixed sneutrinos as thermal dark matter*, *JCAP* **1011** (2010) 017, [[arXiv:1008.0580](#)].
- [63] J. R. Ellis, K. A. Olive, Y. Santoso, and V. C. Spanos, *Update on the direct detection of supersymmetric dark matter*, *Phys.Rev.* **D71** (2005) 095007, [[hep-ph/0502001](#)].
- [64] G. Belanger, F. Boudjema, A. Pukhov, and A. Semenov, *Dark matter direct detection rate in a generic model with micrOMEGAs 2.2*, *Comput.Phys.Commun.* **180** (2009) 747–767, [[arXiv:0803.2360](#)].

- [65] M. Perelstein and B. Shakya, *XENON100 Implications for Naturalness in the MSSM, NMSSM and lambda-SUSY*, [arXiv:1208.0833](#).
- [66] **CMS** Collaboration, S. Chatrchyan *et. al.*, *Observation of a new boson at a mass of 125 GeV with the CMS experiment at the LHC*, *Phys.Lett.B* (2012) [[arXiv:1207.7235](#)].
- [67] **ATLAS** Collaboration, G. Aad *et. al.*, *Observation of a new particle in the search for the Standard Model Higgs boson with the ATLAS detector at the LHC*, *Phys.Lett.B* (2012) [[arXiv:1207.7214](#)].
- [68] **CMS** Collaboration, S. Chatrchyan *et. al.*, *Search for supersymmetry in hadronic final states using  $MT_2$  in  $pp$  collisions at  $\sqrt{s} = 7$  TeV*, [arXiv:1207.1798](#).
- [69] **ATLAS** Collaboration, G. Aad *et. al.*, *Search for squarks and gluinos with the ATLAS detector in final states with jets and missing transverse momentum using  $4.7 \text{ fb}^{-1}$  of  $\sqrt{s} = 7$  TeV proton-proton collision data*, [arXiv:1208.0949](#).
- [70] G. Moortgat-Pick, K. Rolbiecki, and J. Tattersall, *Momentum reconstruction at the LHC for probing CP-violation in the stop sector*, *Phys.Rev.* **D83** (2011) 115012, [[arXiv:1008.2206](#)].
- [71] O. Kittel and A. Pilaftsis, *CP Violation in Correlated Production and Decay of Unstable Particles*, *Nucl.Phys.* **B856** (2012) 682–697, [[arXiv:1108.3314](#)].
- [72] S. Bornhauser, M. Drees, H. Dreiner, O. Eboli, J. Kim, *et. al.*, *CP Asymmetries in the Supersymmetric Trilepton Signal at the LHC*, *Eur.Phys.J.* **C72** (2012) 1887, [[arXiv:1110.6131](#)].
- [73] J. Berger, M. Blanke, Y. Grossman, and S. Ray, *Momentum asymmetries as CP violating observables*, [arXiv:1206.1651](#).
- [74] K. Huitu, J. Laamanen, L. Leinonen, S. K. Rai, and T. Ruppell, *Work in Progress*, .